

Indirect, Direct and Collider Detection of Neutralino Dark Matter in the mSUGRA Model

Howard Baer, Alexander Belyaev, Tadas Krupovnickas and Jorge O’Farrill

Department of Physics, Florida State University Tallahassee, FL 32306, USA
E-mail: baer@hep.fsu.edu, belyaev@hep.fsu.edu
tadas@hep.fsu.edu, ofarrill@hep.fsu.edu

ABSTRACT: We examine the prospects for supersymmetry discovery in the minimal supergravity (mSUGRA) model via indirect detection of neutralino dark matter. We investigate rates for muon detection in neutrino telescopes, and detection of photons, positrons and anti-protons by balloon and space based experiments. We compare the discovery reach in these channels with the reach for direct detection of dark matter, and also with the reach of collider experiments such as Fermilab Tevatron, CERN LHC and a $\sqrt{s} = 0.5 - 1$ TeV linear e^+e^- collider. We pay particular attention to regions of model parameter space in accord with recent WMAP results on the dark matter density of the universe. We find that 3rd generation direct dark matter detection experiments should be able to cover the *entire* WMAP allowed portion of the hyperbolic branch/focus point (HB/FP) region of parameter space, while the IceCube neutrino telescope can cover almost all this region. This is in contrast to the case of the CERN LHC or a linear e^+e^- collider, where only a fraction of the HB/FP region can be accessed. In addition, we show that detection of γ s, e^+ s and \bar{p} s should occur in much of the HB/FP region, as well as in the low $m_{1/2}$ portion of the A annihilation funnel, and will be complementary to searches via colliders in these regions.

KEYWORDS: Supersymmetry Phenomenology, Supersymmetric Standard Model, Dark Matter.

1. Introduction

Evidence for cold dark matter (CDM) in the universe comes from observations of galactic rotation curves and binding of galaxies in clusters, from matching observations of large scale structure with simulations, from gravitational microlensing, from the baryonic density of the universe as determined by Big Bang nucleosynthesis, from observations of supernovae in distant galaxies, and from measurements of anisotropies in the cosmic microwave background radiation (CMB)[1]. In particular, the Wilkinson Microwave Anisotropy Probe (WMAP)[2] collaboration has extracted a variety of cosmological parameters from fits to precision measurements of the CMB radiation. The properties of a flat universe in the standard Λ CDM cosmological model are characterized by the density of baryons (Ω_b), matter density (Ω_m), vacuum energy (Ω_Λ) and the expansion rate (h) which are measured to be:

$$\Omega_b = 0.044 \pm 0.004 \quad (1.1)$$

$$\Omega_m = 0.27 \pm 0.04 \quad (1.2)$$

$$\Omega_\Lambda = 0.73 \pm 0.04 \quad (1.3)$$

$$h = 0.71^{+0.04}_{-0.03}. \quad (1.4)$$

From the WMAP results, a value for the cold dark matter density of the universe can be derived:

$$\Omega_{CDM}h^2 = 0.1126^{+0.0081}_{-0.0090}({}^{+0.0161}_{-0.0181}) \text{ at } 68(95)\% \text{ CL.} \quad (1.5)$$

While the origin of dark energy in the universe remains a conundrum, there exists a number of hypothetical candidate elementary particles to fill the role of CDM.

A particularly attractive candidate for CDM is the lightest neutralino in R -parity conserving supersymmetric models[3]. In the paradigm minimal supergravity (mSUGRA) model[4], it is assumed that at the scale $Q = M_{GUT}$, there is a common scalar mass m_0 , a common gaugino mass $m_{1/2}$, and a common trilinear term A_0 . The soft SUSY breaking terms can be calculated at scale $Q = M_{weak}$ via renormalization group evolution. Electroweak symmetry breaking occurs radiatively (REWSB) due to the large top quark mass, so that the bilinear soft breaking term B can be traded for the weak scale ratio of Higgs vevs $\tan\beta$, and the magnitude (but not the sign) of the superpotential μ term can be specified. Thus, the mSUGRA model is characterized by four parameters plus a sign choice:

$$m_0, m_{1/2}, A_0, \tan\beta, \text{ and } sign(\mu). \quad (1.6)$$

Once these model parameters are specified, then all sparticle masses and mixings are determined, and scattering cross sections may be reliably calculated.

In the early universe at very high temperatures, the lightest neutralino \tilde{Z}_1 will be in thermal equilibrium, so that its number density is well determined. As the universe expands and cools, the expansion rate outstrips the neutralino interaction rate, and a relic density of neutralinos is frozen out. The neutralino relic density $\Omega_{\tilde{Z}_1}h^2$ at the present time can be determined by solving the Boltzmann equation for neutralinos in a Friedmann-Robertson-Walker universe.

In most of the parameter space of the mSUGRA model, it turns out that a value of $\Omega_{\tilde{Z}_1} h^2$ well beyond the WMAP bound is generated. Only certain regions of the mSUGRA model parameter space give rise to a relatively low value of $\Omega_{\tilde{Z}_1} h^2$ in accord with cosmological measurements and theory. These regions consist of:

1. The bulk annihilation region at low values of m_0 and $m_{1/2}$, where neutralino pair annihilation occurs at a large rate via t -channel slepton exchange.
2. The stau co-annihilation region at low m_0 where $m_{\tilde{Z}_1} \simeq m_{\tilde{\tau}_1}$ so that \tilde{Z}_1 s may co-annihilate with $\tilde{\tau}_1$ s in the early universe[5].
3. The hyperbolic branch/focus point (HB/FP) region[6] at large m_0 near the boundary of the REWSB excluded region where $|\mu|$ becomes small, and the neutralinos have a significant higgsino component, which facilitates annihilations to WW and ZZ pairs[7, 8].
4. The A -annihilation funnel, which occurs at very large $\tan\beta \sim 45 - 60$ [9]. In this case, the value of $m_A \sim 2m_{\tilde{Z}_1}$. An exact equality of the mass relation isn't necessary, since the A width can be quite large ($\Gamma_A \sim 10 - 50$ GeV); then $2m_{\tilde{Z}_1}$ can be several widths away from resonance, and still achieve a large $\tilde{Z}_1\tilde{Z}_1 \rightarrow A \rightarrow f\bar{f}$ annihilation cross section. The heavy scalar Higgs H also contributes to the annihilation cross section.

In addition, there exists a region of neutralino top-squark co-annihilation[10] (for very particular A_0 values) and a light Higgs h annihilation funnel[63] (at low $m_{1/2}$ values).

In past years, the bulk annihilation region of parameter space was favored. This situation has changed in that the low m_0 and $m_{1/2}$ portion of the bulk annihilation region has been excluded by LEP2 chargino and Higgs search bounds, while the larger m_0 and $m_{1/2}$ portion generally predicts values of $\Omega_{\tilde{Z}_1} h^2$ beyond the rather restrictive upper bound of $\Omega_{\tilde{Z}_1} h^2 < 0.129$ obtained from WMAP. Any remaining portions of the bulk region give rise to large- usually anomalous- predictions of the rate for $BF(b \rightarrow s\gamma)$ decays and muon anomalous magnetic moment $a_\mu = (g - 2)_\mu/2$ [11, 12]. An increase of either of the parameters m_0 or $m_{1/2}$ leads generally to heavier sparticle masses and m_h values, so that predictions for loop induced processes become more SM-like.

A panoply of collider and non-accelerator experiments are now operating or will soon be deployed that will shed light on CDM. Prospects for detecting dark matter and determining its properties are particularly bright in the case of neutralinos from supersymmetry. Neutralino dark matter may well be produced at the Fermilab Tevatron $p\bar{p}$ collider[13], the CERN LHC[14] pp collider, and a $\sqrt{s} = 0.5 - 1$ TeV linear e^+e^- collider[15]. In addition, there exist both direct and indirect non-accelerator dark matter search experiments that are ongoing and proposed. Direct dark matter detection has been recently examined by many authors[16], and observable signal rates are generally found in either the bulk annihilation region, or in the HB/FP region, while direct detection of DM seems unlikely in the A -funnel or in the stau co-annihilation region.

Indirect detection of neutralino dark matter[17] may occur via

1. observation of high energy neutrinos originating from $\tilde{Z}_1\tilde{Z}_1$ annihilations in the core of the sun or earth[18],
2. observation of γ -rays originating from neutralino annihilation in the galactic core or halo[19] and
3. observation of positrons[20] or anti-protons[21] originating from neutralino annihilation in the galactic halo.

The latter signals would typically be non-directional due to the influence of galactic magnetic fields, unless the neutralino annihilations occur relatively close to earth in regions of clumpy dark matter.

The indirect signals for SUSY dark matter have been investigated in a large number of papers, and computer codes which yield the various signal rates are available[22, 23]. Recent works find that the various indirect signals occur at large rates in the now disfavored bulk annihilation region, and also in the HB/FP region[7]. Naively, this is not surprising since the same regions of parameter space that include large neutralino annihilation cross sections in the early universe should give large annihilation cross sections as sources of indirect signals for SUSY dark matter. In Ref. [24], it was pointed out that the A annihilation funnel can give rise to large rates for cosmic γ s, e^+ s and \bar{p} s. However, neutralino-nucleon scattering cross sections are low in the A annihilation funnel, so that no signal is expected at neutrino telescopes, which depend more on the neutralino-nucleus scattering cross section than on the neutralino annihilation rates. Our goal in this paper is to combine the projected discovery contours from Tevatron, LHC and LC searches with those of direct and indirect dark matter search experiments. It turns out that each distinct region of mSUGRA parameter space which gives rise to an acceptable $\Omega_{\tilde{Z}_1} h^2$ value also gives a set of unique predictions for combinations of collider and non-accelerator experiments.

We begin our analysis by generating sparticle mass spectra using Isajet v7.69[25], which includes full one-loop radiative corrections to all sparticle masses and Yukawa couplings, and minimizes the scalar potential using the renormalization group improved 1-loop effective potential including all tadpole contributions, evaluated at an optimized scale choice which accounts for leading two loop terms. Good agreement between m_h values is found in comparison with the FeynHiggs program, and there is good agreement as well in the m_A calculation between Isajet and SoftSUSY, Spheno and Suspect codes, as detailed in Ref. [26]. To evaluate the indirect signals expected from the mSUGRA model, we adopt the DarkSUSY 3.14 package[23] interfaced to Isasugra¹. For our calculation of the neutralino relic density, we use the IsaReD program[27] interfaced with Isajet. IsaReD calculates all relevant neutralino pair annihilation and co-annihilation processes with relativistic thermal averaging[28]. An important element of the calculation is that IsaReD calculates the neutralino relic density using the Isajet t , b and τ Yukawa couplings evaluated at the scale $Q = m_A$. The Yukawa coupling calculation begins with the \overline{DR}' fermion masses at scale $Q = M_Z$, and evolves via 1-loop SM renormalization group equations (RGEs) to the scale

¹Isasugra is a subprogram of the Isajet package that calculates sparticle mass spectra and branching fractions for a variety of supersymmetric models

$Q_{SUSY} = \sqrt{m_{\tilde{L}} m_{\tilde{R}}}$, where complete MSSM 1-loop threshold corrections are implemented. Evolution at higher mass scales is implemented via 2-loop MSSM RGEs. The final RGE solution is gained after iterative running of couplings and soft terms between M_Z and M_{GUT} and back until a convergent solution is achieved.

The remainder of this paper is organized as follows. In Sec. 2, we present an overview of indirect, direct and collider search experiments for neutralino dark matter. In Sec. 3, we discuss the impact of different halo models on our calculations. We then present our main results, which are a series of plots in the m_0 vs. $m_{1/2}$ plane of the mSUGRA model showing the comparative reach of various indirect, direct and collider searches for neutralino dark matter. In Sec. 4, we present our conclusions.

2. Experimental overview

2.1 Neutrino telescopes

A novel technique for detecting dark matter is to search for neutrino signals coming from neutralino annihilation in the core of the earth or the sun[18]. As the sun or earth proceeds on its orbital path, neutralinos can be swept up and become gravitationally captured by the process of neutralino-nucleon scattering until the recoil neutralino velocity drops below the escape velocity. Thus, a high density of neutralinos can accumulate in the core of the earth or sun, where they can efficiently annihilate. Neutralino annihilation into SM final states such as $b\bar{b}$, $c\bar{c}$, W^+W^- or ZZ ultimately yields neutrinos via the $b \rightarrow c\ell\nu_\ell$, $c \rightarrow s\ell\nu_\ell$, $W \rightarrow \ell\nu$ or $Z \rightarrow \nu_\ell\bar{\nu}_\ell$ decays. The neutrinos can propagate out of the core of the earth or sun, and be detected via $\nu_\mu \rightarrow \mu$ conversions in neutrino telescopes such as Antares or IceCube. In fact, limits have already been obtained by Amanda for the case of neutralino annihilation in the core of the earth[29].

The Antares ν telescope should be sensitive to $E_\mu > 10$ GeV; it is in the process of deployment and is expected to turn on in 2006[30]. It should attain a sensitivity of $100 - 1000 \mu\text{s}/\text{km}^2/\text{yr}$. The IceCube ν telescope is also in the process of deployment at the south pole[31]. It should be sensitive to $E_\mu > 25 - 50$ GeV, and is expected to attain a sensitivity of $40 - 50 \mu\text{s}/\text{km}^2/\text{yr}$. Full deployment of all detector elements is expected to be completed by 2010.

The rate for neutralino annihilation in the sun or earth is given by

$$\Gamma_A = \frac{1}{2}C \tanh^2(t_\odot/\tau), \quad (2.1)$$

where C is the capture rate, A is the total annihilation rate times relative velocity per volume, t_\odot is the present age of the solar system and $\tau = 1/\sqrt{CA}$ is the equilibration time. For the sun, the age of the solar system exceeds the equilibration time, so $\Gamma_A \sim \frac{C}{2}$, and the muon flux tends to follow the neutralino-nucleon scattering rate rather than the neutralino pair annihilation cross section. In this case, the indirect dark matter detection rate should be relatively independent of the dark matter halo profile, aside from the value of the local neutralino relic density. Thus, uncertainties in the predicted rates for neutrino detection via neutralino annihilation in the core of the sun should be low. In contrast to the sun, the

earth has typically a much longer equilibration time τ , so that $\Gamma_A \sim \frac{1}{2}C^2At^2$, and is hence more sensitive to the neutralino annihilation cross section times relative velocity. Muon rates from neutralino annihilation in the core of the earth are typically much lower than those from the sun. In addition, expected rates from the earth may be diminished even further by solar depletion effects: see J. Lundberg and J. Edsjö, Ref. [32] (these effects are not included in DarkSUSY 3.14, but are included in DarkSUSY 4.0).

2.2 Detection of γ s

Neutralinos may also collect in the core of the galaxy, where they can annihilate at a high rate. In this case, $\tilde{Z}_1\tilde{Z}_1 \rightarrow q\bar{q}$, W^+W^- , $ZZ \rightarrow \text{hadrons}$ which gives rise to photons typically from $\pi^0 \rightarrow \gamma\gamma$ decay. It is also possible for $\tilde{Z}_1\tilde{Z}_1 \rightarrow \gamma\gamma$ (or $Z\gamma$), in which case $E_\gamma \simeq m_{\tilde{Z}_1}$. The signature is spectacular in this case, but the rates are loop suppressed. The γ rays can be detected down to sub-GeV energies with space-based detectors such as EGRET[33] or GLAST[34]. Ground based arrays require much higher photon energy thresholds of order 20 – 100 GeV. Experiments such as GLAST should be sensitive to rates of order 10^{-10} γ s/cm²/sec assuming $E_\gamma > 1$ GeV. In fact, it has recently been suggested that the extra-galactic gamma ray background radiation as measured by EGRET is well fit by a model of neutralino annihilation[35]; see also [36]. It is important to note that the prediction for rates for γ detection depends sensitively on models for the neutralino density near the galactic core. The latter quantity is poorly known, so there can be a wide range in predicted rates depending on assumptions about the galactic halo profile.

2.3 Detection of e^+ s

Cosmic positrons may also be searched for from neutralino annihilations in the galactic halo. In this case, the positrons would arise as decay products of heavy quarks, leptons and gauge bosons produced in neutralino annihilations. Space based anti-matter detectors such as Pamela[37] and AMS-02[38] will be able to search for anomalous positron production from dark matter annihilation. The cosmic positron excess as measured by HEAT[39] has been suggested as having a source in galactic halo neutralino annihilations[40, 36]. It is suggested by Feng *et al.*[7] that a reasonable observability criteria is that signal-to-background (S/B) rates should be greater than the 1 – 2% level. To calculate the S/B rates, we adopt fit C from Ref. [7] for the $E^2d\Phi_{e^+}/d\Omega dE$ background rate:

$$E^2d\Phi_{e^+}/d\Omega dE = 1.6 \times 10^{-3} E^{-1.23}, \quad (2.2)$$

where E is in GeV. We compute the signal using the DarkSUSY positron flux evaluated at an “optimized” energy of $E = m_{\tilde{Z}_1}/2$, as suggested in Ref. [7]. A $S/B \sim 0.01$ rate may be detectable[7, 17] by experiments such as Pamela and AMS-02.

2.4 Detection of \bar{p} s

Antiprotons may also be produced in the debris of neutralino annihilations in the galactic halo. Such antiprotons have been measured by the BESS collaboration[41]. The differential flux of antiprotons from the galactic halo, $d\Phi_{\bar{p}}/dE_{\bar{p}}d\Omega$, as measured by BESS, has a peak in

the kinetic energy distribution at $E_{\bar{p}} \sim 1.76$ GeV. The height of the peak at $E_{\bar{p}} \sim 1.76$ GeV is $\sim 2 \times 10^{-6} \bar{p}/\text{GeV}/\text{cm}^2/\text{s}/\text{sr}$. Signal rates in the range of $10^{-7} - 10^{-6} \bar{p}/\text{GeV}/\text{cm}^2/\text{s}/\text{sr}$ might thus provide a benchmark for observability.

2.5 Direct search for neutralino DM

If indeed all space is filled with relic neutralinos, then it may be possible to directly detect them via their scattering from nuclei. Early limits on the spin-independent neutralino-nucleon cross-section (σ_{SI}) have been obtained by the CDMS[42], EDELWEISS[43] and ZEPLIN1[44] groups, while a signal was claimed by the DAMA collaboration[45]. Collectively, we will refer to the reach from these groups as the “Stage 1” dark matter search. Depending on the neutralino mass, the combined limit on σ_{SI} varies from 10^{-5} to 10^{-6} pb. This cross section range is beyond the predicted levels from most supersymmetric models. However, experiments in the near future like CDMS2, CRESST2[46], ZEPLIN2 and EDELWEISS2 (Stage 2 detectors) should have a reach of the order of 10^{-8} pb. In fact, the first results from CDMS2 have recently appeared, and yield a considerable improvement over the above mentioned Stage 1 results[47]. Finally, a number of experiments such as GENIUS[48], ZEPLIN4[49] and XENON[50] are in the planning stage. We refer to these as Stage 3 detectors, which promise impressive limits of the order of $\sigma_{SI} < 10^{-9} - 10^{-10}$ pb, and would allow the exploration of a considerable part of parameter space of many supersymmetric models. In particular, the Stage 3 direct DM detectors should be able to probe almost the entire HB/FP region of mSUGRA model parameter space. We note here in addition that the Warm Argon Program (WARP)[51] promotes a goal of detecting neutralino-nucleus scattering cross sections as low 10^{-11} pb.

2.6 Fermilab Tevatron

The Fermilab Tevatron $p\bar{p}$ collider can search for neutralino dark matter by detecting superparticle production reactions which lead to anomalous missing energy in the final state. For mSUGRA model parameter choices in accord with bounds on the chargino mass from LEP2 ($m_{\tilde{W}_1} > 103.5$ GeV), the most promising discovery channel is the clean trilepton plus \cancel{E}_T final state[52], which typically originates from $p\bar{p} \rightarrow \tilde{W}_1 \tilde{Z}_2 X \rightarrow 3\ell + \cancel{E}_T + X$, where X stands for assorted hadronic debris, and where the trileptons tend to originate from $\tilde{W}_1 \rightarrow \ell\nu_\ell \tilde{Z}_1$ and $\tilde{Z}_2 \rightarrow \ell\bar{\ell} \tilde{Z}_1$ decay. Trilepton signal rates and backgrounds have been calculated in Ref. [53] using cuts SC2. These results were updated and extended to large m_0 regions of parameter space in Ref. [54].

2.7 CERN LHC

The CERN LHC can search for neutralino dark matter by detecting superparticle production reactions which lead to anomalous missing energy in the final state. For LHC, however, gluino and squark production reactions are expected to be the dominant SUSY cross sections. The gluinos and squarks can decay through possibly lengthy cascade decays so that signal events will consist of multi-jets plus isolated leptons plus \cancel{E}_T [55]. Signal and background levels have been computed in Ref. [56] for various combinations of jet and

lepton cuts. We adopt the most recent calculations of Baer *et al.*[56] for our projections of the LHC reach, assuming 100 fb^{-1} of integrated luminosity.

2.8 Linear e^+e^- collider

A linear e^+e^- collider operating at CM energy $\sqrt{s} = 0.5 - 1 \text{ TeV}$ can also search for neutralino dark matter by detecting superparticle production reactions which lead to anomalous missing energy in the final state. The ultimate reach limits in the mSUGRA model depend on which sparticles are kinematically accessible to production. The reach contours are determined by[57, 58]

- $e^+e^- \rightarrow \tilde{\ell}^+\tilde{\ell}^-$ at low m_0 , followed typically by $\tilde{\ell} \rightarrow \ell\tilde{Z}_1$ decay and
- $e^+e^- \rightarrow \tilde{W}_1^+\tilde{W}_1^-$ production at moderate to high m_0 values, where typically $\tilde{W}_1 \rightarrow f\tilde{f}'\tilde{Z}_1$ or $W\tilde{Z}_1$ (f is any SM fermion).
- In intermediate regions, $e^+e^- \rightarrow \tilde{Z}_1\tilde{Z}_2$ and/or $e^+e^- \rightarrow ZH, Ah$ may be accessible.

In the HB/FP region, the superpotential μ parameter becomes small, and the \tilde{W}_1 and \tilde{Z}_1 become increasingly higgsino like, and nearly mass degenerate. In the small mass gap region, conventional cuts oriented towards a substantial $m_{\tilde{W}_1} - m_{\tilde{Z}_1}$ mass gap must be replaced by new cuts. Ultimately, an e^+e^- LC should be able to see chargino pairs essentially up to the kinematic limit for their production, over all of mSUGRA parameter space. Reach plots have been presented in Ref. [58] assuming 100 fb^{-1} of integrated luminosity for both the $\sqrt{s} = 0.5 \text{ TeV}$ and 1 TeV machines.

3. Direct, indirect and collider searches in the mSUGRA model

In this section, we evaluate the reach of various indirect, direct and collider searches for neutralino dark matter in the mSUGRA model. For our predictions of indirect neutralino detection rates, we use the DarkSUSY program[23], modified to interface with Isajet v7.69. The Isajet subprogram Isasugra is used to predict the sparticle mass spectrum and decay widths for various supersymmetric models, including mSUGRA.

3.1 Calculational overview and dependence on halo model

While predictions for the reach of colliders for neutralino dark matter are firmly grounded in perturbative quantum field theory, many of the predictions for direct and indirect detection of dark matter depend on the assumed density profile of the galactic halo.

For halo model dependence in the distribution of dark matter, we adopt the default DarkSUSY value: a spherically symmetric isothermal distribution given by

$$\rho(r) = \rho_0 \frac{(r/r_0)^{-\gamma}}{(1 + (r/a)^\alpha)^{\frac{\beta-\gamma}{\alpha}}} (1 + (r_0/a)^\alpha)^{\frac{\beta-\gamma}{\alpha}} \quad (3.1)$$

where $(\alpha, \beta, \gamma) = (2, 2, 0)$, $r_0 = 8.5 \text{ kpc}$ is the distance of earth to the galactic center, $\rho_0 = 0.3 \text{ GeV/cm}^3$ is the local dark matter density and $a = 3.5 \text{ kpc}$ is a distance scale. A number of other halo profiles are available in DarkSUSY, including

- Navarro, Frenk, White profile with $a = 20$ kpc, with $(\alpha, \beta, \gamma) = (1, 3, 1)$ [59],
- Moore *et al.* profile with $a = 28$ kpc, with $(\alpha, \beta, \gamma) = (1.5, 3, 1.5)$ [60] and
- Kravtsov *et al.* profile with $\rho_0 = 0.6$ GeV/cm³, $a = 10$ kpc, with $(\alpha, \beta, \gamma) = (2, 3, 0.4)$ [61].

The alternative distributions all use $r_0 = 8.0$ kpc as the sun galactocentric distance value.

In Fig. 1, we show in frame *a*) the various halo model distributions. While the distributions are in close accord at $r = 8.5$ kpc (the distance of the sun to the galactic center), the profiles disagree strongly as $r \rightarrow 0$, reflecting our relative ignorance of the density of dark matter expected near the galactic center. In frame *b*), we show the neutralino relic density versus mSUGRA parameter m_0 , with $m_{1/2} = 550$ GeV, $A_0 = 0$, $\mu < 0$ and $\tan \beta = 50$. The horizontal line shows the WMAP upper bound on $\Omega_{\tilde{Z}_1} h^2$. In frame *c*), we show the flux of muons with $E_\mu > 25$ GeV originating from neutralino annihilation to neutrinos in the core of the sun. These curves only depend on the *local* neutralino relic density, and not on the global galactic halo profile. Thus, the first three halo profiles yield the same predictions for the muon detection rate, while the Kravtsov distribution, with a higher value for the local relic density, also gives higher rates for neutrino telescopes. In frame *d*), we show the flux of photons Φ_γ (γ s/cm²/sec) with $E_\gamma > 1$ GeV emanating from the galactic center, within a cone of solid angle 0.001 sr. The rates are large at large m_0 in the HB/FP region[7], and are also large at $m_0 \sim 1000$ GeV, where neutralino annihilation in the galactic core can occur through the A and H resonances[24]. Overall, the predicted rates at fixed m_0 vary over several orders of magnitude, reflecting the different model predictions for the DM density at the galactic center. In frame *e*), we show as well the expected positron signal-to-background (S/B) rate for positrons originating in neutralino annihilations in the galactic halo. We see that observable rates may again occur in the HB/FP region, and also in the A -annihilation funnel. However, the uncertainty in the predictions due to variation in the halo model is less severe than in the γ case, since now the positrons are expected to arise relatively nearby in the galaxy, where the DM density is much more constrained. In frame *f*), we show the differential flux of antiprotons from the galactic halo, $d\Phi_{\bar{p}}/dE_{\bar{p}}d\Omega$, for $E_{\bar{p}} = 1.76$ GeV, which is near the location of the peak in the \bar{p} kinetic energy distribution as measured by the BESS collaboration[41]. We see from the figure that the largest rates occur in the HB/FP region, and also in the A -annihilation funnel; in these regions, the signal rates can extend into the region of observability. Again, the predicted rates are sensitive to the assumed halo model. We note, however, that the DarkSUSY default halo distribution tends to give the most conservative of rate predictions, and it is possible that indirect detection rates could be much higher than those shown using the default halo model.

One final qualifying note: it is common practice to rescale direct or indirect detection rates by a factor $\Omega_{\tilde{Z}_1} h^2 / (\Omega_{CDM} h^2)_{ref}$ when $\Omega_{\tilde{Z}_1} h^2 < (\Omega_{CDM} h^2)_{ref}$, where $(\Omega_{CDM} h^2)_{ref}$ is some reference value $\sim 0.025 - 0.1$ which would give rise to the assumed local dark matter density $\rho = 0.3$ GeV/cm³. We do not apply this practice here. It is possible in a variety

of non-standard cosmological models (such as those containing quintessential scalar fields or primordial anisotropies) to obtain a dark matter relic density much higher than that obtained in a Λ CDM model. See *e.g.* Ref. [62] for details.

3.2 Results for the mSUGRA model

Our first results for the mSUGRA model are shown in Fig. 2 in the m_0 vs. $m_{1/2}$ plane for $\tan\beta = 10$, $A_0 = 0$ and $\mu > 0$. We take $m_t = 175$ GeV. The left-most red region is excluded because the stau becomes the LSP (in violation of search limits for stable charged or colored relics from the Big Bang), while the right-most red region is excluded due to a lack of REWSB. The lower yellow region is excluded by LEP2 searches for chargino pair production ($m_{\tilde{W}_1} > 103.5$ GeV), while the region below the yellow contour is excluded by LEP2 Higgs searches ($m_h > 114.4$ GeV for a SM-like Higgs boson). The green shaded region has $\Omega_{\tilde{Z}_1} h^2 < 0.129$, in accord with the upper bound on CDM from WMAP. The left-most green strip along the low m_0 excluded region is the stau co-annihilation corridor, while the right-most green region corresponds to the HB/FP region. A remaining green region sitting just atop the LEP2 excluded region is the light Higgs annihilation corridor, where $2m_{\tilde{Z}_1} \sim m_h$ [63]. The uncolored regions all give too large a CDM relic density, and are thus excluded.

The Fermilab Tevatron reach contour corresponding to a 5σ signal for 10 fb^{-1} of integrated luminosity is denoted by TEV, while the CERN LHC 5σ reach for 100 fb^{-1} is denoted LHC. The reach of a $\sqrt{s} = 500$ GeV and 1000 GeV linear collider is denoted by LC500 and LC1000, respectively, assuming 100 fb^{-1} for each. We see from the figure that the Tevatron can cover the light Higgs annihilation corridor, while the LC1000 and LHC can cover the stau co-annihilation region. The LHC can cover the HB/FP region up to $m_{1/2} \sim 700$ GeV, which corresponds to a reach in $m_{\tilde{g}}$ of about 1.8 TeV. In this region, squarks and sleptons are 4-7 TeV in mass, and effectively decoupled from LHC production. LHC can generate an observable signal cross section provided $m_{\tilde{g}}$ is light enough. If $m_{\tilde{g}}$ is too heavy ($\gtrsim 1.8$ TeV), then $pp \rightarrow \tilde{g}\tilde{g}X$ occurs at too low of a rate. Charginos and neutralinos can be quite light in the HB/FP region since $|\mu|$ is small, but their signal events are difficult for LHC to extract from background, owing in part to a decreasing $m_{\tilde{W}_1} - m_{\tilde{Z}_1}$ mass gap as $|\mu|$ decreases. The LC500 and LC1000 can still generate $\tilde{W}_1^+ \tilde{W}_1^-$ pairs in the HB/FP region if they are kinematically accessible, and should be able to extract the corresponding low energy release events above SM background[58]. In the HB/FP region, we have the unusual situation that the LC reach exceeds that of the CERN LHC. However, the high $m_{1/2}$ portion of the HB/FP region gives rise to cases where the chargino mass is too heavy to be accessible by a $\sqrt{s} = 1$ TeV LC, so a thorough search for SUSY by colliders in this DM allowed region apparently can't be made (unless a higher energy LC is constructed).

We also show contours of

- Stage 3 direct detection experiments ($\sigma_{SI} > 10^{-9}$ pb; black contour),
- reach of IceCube ν telescope with $\Phi^{sun}(\mu) = 40 \mu\text{s}/\text{km}^3/\text{yr}$ and $E_\mu > 25$ GeV (magenta contour),

- the $\Phi(\gamma) = 10^{-10} \text{ } \gamma\text{s/cm}^2\text{/s}$ contour with $E_\gamma > 1 \text{ GeV}$ in a cone of 0.001 sr directed at the galactic center (dark blue contour),
- the $S/B > 0.01$ contour for halo produced positrons (blue-green contour) and
- the antiproton flux rate $\Phi(\bar{p}) = 3 \times 10^{-7} \text{ } \bar{p}\text{s/cm}^2\text{/s/sr}$ (lavender contour).

As noted by Feng *et al.*[7], *all* these indirect signals are visible inside some portion of the HB/FP region, while *none* are visible in generic DM disallowed regions (under the assumed smooth halo profiles). The intriguing point is that almost the entire HB/FP region (up to $m_{1/2} \sim 1400 \text{ GeV}$) can be explored by the cubic km scale IceCube ν telescope! It can also be explored (apparently at later times) by the Stage 3 direct DM detectors. Given the relative time scales of the various search experiments, if SUSY lies within the upper HB/FP region, then it may well be discovered first by IceCube (and possibly Antares), with a signal being later confirmed by direct DM detection and possibly the TeV scale linear e^+e^- collider. There is also some chance to obtain indirect γ , e^+ and \bar{p} signals in this region. Notice that if instead SUSY lies within the stau co-annihilation corridor, then it will be easily discovered by the LHC (for $\tan\beta = 10$), but all indirect detection experiments will find null results in their DM searches.

In Fig. 3, we show again the m_0 *vs.* $m_{1/2}$ plane, but this time for $\tan\beta = 30$ (other parameters remain the same). The results are rather similar to the $\tan\beta = 10$ case shown in Fig. 2, although the stau annihilation corridor has expanded somewhat to higher $m_{1/2}$ values, and also the low m_0 and $m_{1/2}$ (bulk) region of parameter space has become more accessible to direct DM searches and even indirect DM searches in the \bar{p} channel. The CERN LHC can still cover the entire stau co-annihilation region, and the low $m_{1/2}$ portion of the HB/FP region. The LC1000 can cover much of the stau co-annihilation region and much of the high $m_{1/2}$ HB/FP region. However, a search of the $m_{1/2} < 1400 \text{ GeV}$ portion of the HB/FP region can be made by the IceCube neutrino telescope, and later, Stage 3 direct DM search experiments can cover the entire region.

Fig. 4 shows the m_0 *vs.* $m_{1/2}$ plane for an even higher $\tan\beta = 52$ value. In this case, the stau co-annihilation corridor has increased to well beyond the LHC reach, and in fact this region of mSUGRA parameter space appears to be one which is consistent with WMAP relic density bounds, but beyond reach of *any* of the planned collider, direct or indirect search experiments for neutralino dark matter. At this high of a $\tan\beta$ value, the value of pseudoscalar Higgs mass m_A has dropped[64] to such a level that there exists a large amplitude for off mass shell $\tilde{Z}_1\tilde{Z}_1 \rightarrow A^* \rightarrow b\bar{b}$ annihilation in the early universe[8]. This additional amplitude helps to amplify the low m_0 DM allowed region, where now a combination of slepton co-annihilation, off shell A , H resonance annihilation, and t -channel neutralino annihilation via relatively light sfermions all serve to expand the DM allowed region. However, the HB/FP region is relatively insensitive to changes in $\tan\beta$, and is still well covered by ν -telescopes and direct DM searches. The reach of direct DM search experiments has vastly increased in the low m_0 and $m_{1/2}$ regions, where the reach of Stage 3 detectors is comparable to the LC1000. The increase in direct DM detection rates is due to enhanced scattering via t -channel Higgs exchange graphs; these are proportional to the

square of b and τ Yukawa couplings, which are large at large $\tan\beta$ [8]. In addition, at low m_0 and $m_{1/2}$, the DM allowed region may give rise to detectable rates for γ , \bar{p} and e^+ detection.

Fig. 5 shows the m_0 vs. $m_{1/2}$ plane for $\tan\beta = 55$. In this case, the A annihilation funnel has moved into the central part of parameter space, opening up a large new region that gives a neutralino relic density in accord with WMAP results[9]. The A annihilation funnel extends beyond the 100 fb^{-1} reach of the LHC, and makes a case for LHC running with much higher integrated luminosities, if no physics beyond the SM is found. In addition, the searches for γ s, e^+ s and \bar{p} s are all enhanced in this region, since now halo neutralinos can also annihilate through the broad A and H resonances[24]. Searches in these channels, however, cover only the low $m_{1/2}$ portion of the A annihilation funnel. Annihilation through the A funnel also serves to expand somewhat the breadth of the HB/FP region. Even so, most of the HB/FP region can still be covered by the IceCube ν telescope, while Stage 3 DM detectors can cover the entire region. Much of it can also be covered by LHC, LCs and the search for halo annihilations into γ s, e^+ s and \bar{p} s. As $\tan\beta$ increases much beyond 55, the parameter space starts to collapse due to inappropriate breakdown of EW symmetry.

In Fig. 6, we show the m_0 vs. $m_{1/2}$ plane for $\mu < 0$, $A_0 = 0$ and $\tan\beta = 45$. For negative μ values, the A -annihilation funnel enters the plane at lower $\tan\beta$ values; it is hence narrower than in Fig. 5, since the b and τ Yukawa couplings are smaller, and the A and H widths not so wide. In this case, the CERN LHC covers almost all the stau co-annihilation region and the A funnel, and would certainly cover all of these with a higher integrated luminosity. As before, the HB/FP region is only partially covered by LHC and also by a LC, but again it is covered by the IceCube ν telescope up to $m_{1/2} \sim 1400 \text{ GeV}$, and covered completely by Stage 3 direct DM detectors. In addition, the enhanced rates for γ s, e^+ s and \bar{p} s are displayed in the A annihilation funnel.

We show in Fig. 7 the same m_0 vs. $m_{1/2}$ plane for $\mu < 0$, but this time for $\tan\beta = 50$. In this case, the A annihilation funnel is more centrally located, and shows observable rates for γ s, e^+ s and \bar{p} s for the lower portion of the funnel. The red bulge moving into the figure at low m_0 and low $m_{1/2}$ denotes the region where $m_A^2 < 0$, and begins the collapse of parameter space at high $\tan\beta$. The HB/FP region is again almost completely covered by IceCube, although the low $m_{1/2}$ portion of this region is no longer accessible to direct DM searches, owing to interferences in the neutralino-proton scattering rates.

4. Conclusions

In previous reports, the reach of the Fermilab Tevatron, the CERN LHC and $\sqrt{s} = 0.5$ and 1 TeV e^+e^- linear colliders has been computed in the mSUGRA model. In addition, the reach of direct DM detection experiments has also been worked out, and found to be in many respects complementary to collider searches[65]. In this paper, we augment these previous works by presenting as well the reach of various indirect search experiments for neutralino dark matter. These include searches for neutralino annihilation in the core of the sun (or earth), leading to detection of $\nu_\mu \rightarrow \mu$ conversions in neutrino telescopes such as Antares and IceCube. Also, we show reach contours for indirect searches for neutralino

annihilation in the galactic core via γ detection, and for neutralino annihilation in the galactic halo via e^+ and \bar{p} detection. Our results have focussed mainly on the WMAP allowed regions of the paradigm mSUGRA model.

We have several main conclusions:

1. In the stau co-annihilation region, indirect searches for neutralino dark matter have only a feeble reach. The best reach comes if $\tan\beta$ is large and there is some overlap with the A annihilation funnel. However, the CERN LHC can probe *all* the stau coannihilation region for $\tan\beta \lesssim 45$. Much of it can also be explored by linear e^+e^- colliders. In fact, the large $m_{1/2}$ portion of this region at large $\tan\beta$ seems to be a region of mSUGRA parameter space which is consistent with WMAP limits on $\Omega_{\tilde{Z}_1} h^2$, but not accessible to any planned experiments.
2. Most of the A annihilation funnel can be explored by the CERN LHC, although again the large $m_{1/2}$ portion of it might not be accessible to any search experiments. The lower portion of the A funnel is also accessible to γ , e^+ and \bar{p} searches for neutralino annihilation in the galactic core or halo. The indirect detection reach in this region is comparable to that of a $\sqrt{s} = 1$ TeV linear e^+e^- collider. Detection of $\nu_\mu \rightarrow \mu$ in neutrino telescopes is *unlikely* to occur in this region.
3. In the HB/FP region, the CERN LHC can cover $m_{1/2}$ values up to ~ 700 GeV, corresponding to a value of $m_{\tilde{g}} \sim 1.8$ TeV. Linear e^+e^- collider can do better, since they can detect chargino pair production, even if the energy release from chargino 3-body decay is very low. The LC reach is limited by their CM energy, and a 1 TeV linear collider will not be quite sufficient to explore the entire high $m_{1/2}$ portion of the HB/FP region. However, in this region, rates for detection of neutrinos arising from neutralino annihilation in the core of the sun are large, and it seems likely that IceCube can explore or rule out the HB/FP region for $m_{1/2} < 1400$ GeV. In addition, Stage 3 direct DM detection experiments sensitive to neutralino proton spin-independent scattering cross sections of 10^{-9} pb should be able to access the entire HB/FP region, unless $\mu < 0$ and $\tan\beta$ is large, in which case a small hole arises in the low $m_{1/2}$ portion (which will be explored by LHC and LC anyway).

Ultimately, the search for neutralino dark matter can proceed via direct DM searches, indirect DM searches and collider searches. By combining results, all the different search experiments can cover almost all the WMAP allowed mSUGRA model parameter space, save for a few regions which occur in the high $m_{1/2}$ portion of the stau coannihilation corridor or the A annihilation funnel.

Note added: A similar study of indirect and direct signals for neutralino dark matter in the mSUGRA model appeared shortly before the release of this work by Edsjö, Schelke and Ullio[66]. Where the two papers overlap, we seem to be in agreement.

Acknowledgments

We thank X. Tata for conversations. This research was supported in part by the U.S. Department of Energy under contract number DE-FG02-97ER41022.

References

- [1] For recent reviews, see *e.g.* W. Freedman and M. Turner, *Rev. Mod. Phys.* **75** (2003) 1433; A. Lahanas, N. Mavromatos and D. Nanopoulos, *Int. J. Mod. Phys. D* **12** (2003) 1529.
- [2] D. N. Spergel *et al.*, [astro-ph/0302209](#); C. L. Bennett *et al.*, [astro-ph/0302207](#).
- [3] H. Goldberg, *Phys. Rev. Lett.* **50** (1419) 1983; J. Ellis, J. Hagelin, D. Nanopoulos and M. Srednicki, *Phys. Lett.* **B127**, 233 (1983); J. Ellis, J. Hagelin, D. Nanopoulos, K. Olive and M. Srednicki, *Nucl. Phys.* **B238**, 453 (1984).
- [4] A. Chamseddine, R. Arnowitt and P. Nath, *Phys. Rev. Lett.* **49** (1982) 970; R. Barbieri, S. Ferrara and C. Savoy, *Phys. Lett.* **B 119** (1982) 343; N. Ohta, *Prog. Theor. Phys.* **70** (1983) 542; L. J. Hall, J. Lykken and S. Weinberg, *Phys. Rev. D* **27** (1983) 2359; for reviews, see H. P. Nilles, *Phys. Rep.* **110** (1984) 1, and P. Nath, [hep-ph/0307123](#).
- [5] J. Ellis, T. Falk and K. Olive, *Phys. Lett.* **B 444** (1998) 367; J. Ellis, T. Falk, K. Olive and M. Srednicki, *Astropart. Phys.* **13** (2000) 181; M.E. Gómez, G. Lazarides and C. Pallis, *Phys. Rev. D* **61** (2000) 123512 and *Phys. Lett.* **B 487** (2000) 313; R. Arnowitt, B. Dutta and Y. Santoso, *Nucl. Phys.* **B 606** (2001) 59
- [6] K. L. Chan, U. Chattopadhyay and P. Nath, *Phys. Rev. D* **58** (1998) 096004. J. Feng, K. Matchev and T. Moroi, *Phys. Rev. Lett.* **84** (2000) 2322 and *Phys. Rev. D* **61** (2000) 075005; see also H. Baer *et al.*, Ref. [56].
- [7] J. Feng, K. Matchev and F. Wilczek, *Phys. Lett.* **B 482** (2000) 388 and *Phys. Rev. D* **63** (2001) 045024.
- [8] H. Baer and M. Brhlik, *Phys. Rev. D* **57** (1998) 567.
- [9] M. Drees and M. Nojiri, *Phys. Rev. D* **47** (1993) 376; H. Baer and M. Brhlik, *Phys. Rev. D* **53** (1996) 597 and Ref. [8]; H. Baer, M. Brhlik, M. Diaz, J. Ferrandis, P. Mercadante, P. Quintana and X. Tata, *Phys. Rev. D* **63** (2001) 015007; J. Ellis, T. Falk, G. Ganis, K. Olive and M. Srednicki, *Phys. Lett.* **B 510** (2001) 236; L. Roszkowski, R. Ruiz de Austri and T. Nihei, *J. High Energy Phys.* **0108** (024) 2001. A. Lahanas and V. Spanos, *Eur. Phys. J. C* **23** (2002) 185.
- [10] C. Böhm, A. Djouadi and M. Drees, *Phys. Rev. D* **30** (2000) 035012; J. R. Ellis, K. A. Olive and Y. Santoso, *Astropart. Phys.* **18** (2003) 395; J. Edsjö, *et al.*, *JCAP* **04** (2003) 001
- [11] See *e.g.* H. Baer, C. Balazs, A. Belyaev, J. Mizukoshi, X. Tata and Y. Wang, *J. High Energy Phys.* **0207** (2002) 050.
- [12] H. Baer and C. Balazs, *JCAP***05**, (2003) 054, [[hep-ph/0303114](#)].
- [13] H. Baer, T. Krupovnickas and X. Tata, *J. High Energy Phys.* **0307** (020) 2003.
- [14] H. Baer, C. Balazs, A. Belyaev, T. Krupovnickas and X. Tata, *J. High Energy Phys.* **0306** (054) 2003.
- [15] H. Baer, A. Belyaev, T. Krupovnickas and X. Tata, [hep-ph/0311351](#) (2003).
- [16] For a recent analysis, see H. Baer, C. Balazs, A. Belyaev and J. O’Farrill, *JCAP***0309**, 2003 (007); a subset of earlier work includes M. Goodman and E. Witten, *Phys. Rev. D* **31** (1985) 3059; K. Griest, *Phys. Rev. Lett.* **61** (1988) 666 and *Phys. Rev. D* **38** (1988) 2357 [Erratum-*ibid.* *D* **39**, 3802 (1989)]; M. Drees and M. Nojiri, *Phys. Rev. D* **47** (1993) 4226 and *Phys. Rev. D* **48** (1993) 3483; V. A. Bednyakov, H. V. Klapdor-Kleingrothaus and

- S. Kovalenko, *Phys. Rev. D* **50** (1994) 7128; P. Nath and R. Arnowitt, *Phys. Rev. Lett.* **74** (1995) 4592; L. Bergstrom and P. Gondolo, *Astropart. Phys.* **5** (1996) 263; H. Baer and M. Brhlik, *Phys. Rev. D* **57** (1998) 567; J. Ellis, A. Ferstl and K. Olive, *Phys. Lett. B* **481** (2000) 304 and *Phys. Rev. D* **63** (2001) 065016; E. Accomando, R. Arnowitt, B. Dutta and Y. Santoso, *Nucl. Phys. B* **585** (2000) 124; A. Bottino, F. Donato, N. Fornengo and S. Scopel, *Phys. Rev. D* **63** (2001) 125003; M. E. Gomez and J. D. Vergados, *Phys. Lett. B* **512** (2001) 252; A. B. Lahanas, D. V. Nanopoulos and V. C. Spanos, *Phys. Lett. B* **518** (2001) 94; A. Corsetti and P. Nath, *Phys. Rev. D* **64** (2001) 115009; E. A. Baltz and P. Gondolo, *Phys. Rev. Lett.* **86** (2001) 5004; M. Drees, Y. G. Kim, T. Kobayashi and M. M. Nojiri, *Phys. Rev. D* **63** (2001) 115009; see also J. Feng, K. Matchev and F. Wilczek, Ref. [7]; J. R. Ellis, A. Ferstl, K. A. Olive and Y. Santoso, *Phys. Rev. D* **67** (2003) 123502; J. R. Ellis, K. A. Olive, Y. Santoso and V. C. Spanos, *Phys. Rev. D* **69** (2004) 015005; see C. Munoz, hep-ph/0309346 for a recent review.
- [17] For a review, see *e.g.* G. Eigen, R. Gaitskell, G. Kribs and K. Matchev, hep-ph/0112312; see also D. Hooper and L. T. Wang, *Phys. Rev. D* **69** (2004) 035001; W. de Boer, M. Herold, C. Sander and V. Zhukov, hep-ph/0309029.
- [18] J. Silk, K. Olive and M. Srednicki, *Phys. Rev. Lett.* **55** (1985) 257; K. Freese, *Phys. Lett. B* **167** (1986) 295; L. Krauss, M. Srednicki and F. Wilczek, *Phys. Rev. D* **33** (1986) 2079; V. Berezhinsky, A. Bottino, J. R. Ellis, N. Fornengo, G. Mignola and S. Scopel, *Astropart. Phys.* **5** (1996) 333; L. Bergstrom, J. Edsjo and P. Gondolo, *Phys. Rev. D* **55** (1997) 1765 and *Phys. Rev. D* **58** (1998) 103519; A. Bottino, F. Donato, N. Fornengo and S. Scopel, *Astropart. Phys.* **10** (1999) 203; A. Corsetti and P. Nath, *Int. J. Mod. Phys. A* **15** (2000) 905; V. Barger, F. Halzen, D. Hooper and C. Kao, *Phys. Rev. D* **65** (2002) 075022; V. Bertin, E. Nezri and J. Orloff, *Eur. Phys. J. C* **26** (2002) 111 and *J. High Energy Phys.* **0302** (2003) 046.
- [19] F. Stecker, *Phys. Lett. B* **201** (1988) 529; F. W. Stecker and A. J. Tylka, *Astrophys. J.* **343** (1989) 169; S. Rudaz and F. Stecker, *Astrophys. J.* **368** (1991) 406; M. Urban *et al.*, *Phys. Lett. B* **293** (1992) 149; V. Berezhinsky, A. Gurevich and K. Zybin, *Phys. Lett. B* **294** (1992) 221; V. Berezhinsky, A. Bottino and G. Mignola, *Phys. Lett. B* **325** (1994) 136; L. Bergstrom, P. Ullio and J. H. Buckley, *Astropart. Phys.* **9** (1998) 137; L. Bergstrom, J. Edsjö and P. Ullio, *Phys. Rev. D* **58** (1998) 083507; J. Buckley *et al.*, astro-ph/0201160; P. Ullio, L. Bergstrom, J. Edsjö and C. Lacey, *Phys. Rev. D* **66** (2002) 123502.
- [20] S. Rudaz and F. Stecker, *Astrophys. J.* **325** (1988) 16; A. Tylka, *Phys. Rev. Lett.* **63** (1989) 840; M. Turner and F. Wilczek, *Phys. Rev. D* **42** (1990) 1001; M. Kamionkowski and M. Turner, *Phys. Rev. D* **43** (1991) 1774; A. Moskalenko and A. Strong, *Phys. Rev. D* **60** (1999) 063003; E. Baltz and J. Edsjö, *Phys. Rev. D* **59** (1999) 023511; G. Kane, L. T. Wang and J. Wells, *Phys. Rev. D* **65** (2002) 057701; E. Baltz, J. Edsjo, K. Freese and P. Gondolo, *Phys. Rev. D* **65** (2002) 063511; G. Kane, L. T. Wang and T. Wang, *Phys. Lett. B* **536** (2002) 263; D. Hooper, J. Taylor and J. Silk, hep-ph/0312076.
- [21] F. Stecker, S. Rudaz and T. Walsh, *Phys. Rev. Lett.* **55** (1985) 2622; F. Stecker and A. J. Tylka, *Astrophys. J.* **336** (1989) L51; P. Chardonnet, Mignola, P. Salati and R. Taillet, *Phys. Lett. B* **384** (1996) 161; A. Bottino, F. Donato, N. Fornengo and P. Salati, *Phys. Rev. D* **58** (1998) 123503; L. Bergstrom, J. Edsjo and P. Ullio, *Astrophys. J.* **526** (1999) 215.
- [22] neutdriver, by G. Jungman, M. Kamionkowski and K. Griest, see *Phys. Rept.* **267** (1996) 195.
- [23] P. Gondolo, J. Edsjo, P. Ullio, L. Bergstrom, M. Schelke and E. A. Baltz, astro-ph/0211238.

- [24] H. Baer and J. O’Farrill, *JCAP***03**, 012 (2004).
- [25] ISAJET v7.69, by H. Baer, F. Paige, S. Protopopescu and X. Tata, [hep-ph/0312045](#).
- [26] B. Allanach, S. Kraml and W. Porod, *J. High Energy Phys.* **0303** (2003) 016.
- [27] H. Baer, C. Balazs and A. Belyaev, *J. High Energy Phys.* **0203** (2002) 042 and [hep-ph/0211213](#).
- [28] P. Gondolo and G. Gelmini, *Nucl. Phys.* **B 360** (1991) 145; H. Baer and M. Brhlik, *Phys. Rev.* **D 52** (1995) 5031; J. Edsjo and P. Gondolo, *Phys. Rev.* **D 56** (1997) 1879.
- [29] J. Ahrens *et al.* (Amanda Collaboration), *Phys. Rev.* **D 66** (2002) 032006.
- [30] E. Carmona *et al.*, (Antares Collaboration), *Nucl. Phys.* **95** (*Proc. Suppl.*) (2001) 161.
- [31] J. Ahrens *et al.*, (IceCube Collaboration), *Nucl. Phys.* **118** (*Proc. Suppl.*) (2003) 388; F. Halzen, [astro-ph/0311004](#); F. Halzen and D. Hooper, *JCAP***0401** (2004) 002.
- [32] J. Lundberg and J. Edsjö, *Phys. Rev.* **D 69** (2004) 123505.
- [33] H. A. Mayer-Hasselwander *et al.* (EGRET Collaboration), MPE-440 (1998).
- [34] A. Morselli *et al.*, (GLAST Collaboration), *Nucl. Phys.* **113** (*Proc. Suppl.*) (2002) 213.
- [35] D. Elsässer and K. Mannheim, [astro-ph/0405235](#).
- [36] W. de Boer, M. Herold, C. Sander and V. Zhukov, [hep-ph/0312037](#).
- [37] M. Pearce (Pamela Collaboration), *Nucl. Phys.* **113** (*Proc. Suppl.*) (2002) 314.
- [38] J. Casaus *et al.* (AMS Collaboration), *Nucl. Phys.* **114** (*Proc. Suppl.*) (2003) 259.
- [39] M. A. DuVernois *et al.* (HEAT Collaboration), *Astrophys. J.* **559** (2001) 296.
- [40] E. Baltz, J. Edsjö, K. Freese and P. Gondolo, *Phys. Rev.* **D 65** (2002) 063511; see also D. Hooper, J. E. Taylor and J. Silk, [hep-ph/0312076](#).
- [41] S. Orito *et al.* (BESS Collaboration), *Phys. Rev. Lett.* **84** (2000) 1078.
- [42] D. Abrams *et al.* (CDMS Collaboration), *Phys. Rev.* **D 66** (2002) 122003.
- [43] A. Benoit *et al.* (Edelweiss Collaboration), *Phys. Lett.* **B 545** (2002) 43.
- [44] N. Spooner *et al.* (Zeplin-1 Collaboration), in *Proc. of the APS/DPF/DPB Summer Study on the Future of Particle Physics (Snowmass 2001)* ed. N. Graf, eConf **C010630**, E601 (2001).
- [45] R. Bernabei *et al.* (DAMA Collaboration), [astro-ph/0305542](#).
- [46] M. Bravin *et al.* (CRESST Collaboration), *Astrophys. J.* **12** (1999) 107.
- [47] D. S. Akerib *et al.* (CDMS Collaboration), [astro-ph/0405033](#) (2004).
- [48] H. V. Klapdor-Kleingrothaus, A. Dietz and I. V. Krivosheina, *Nucl. Phys.* **124** (*Proc. Suppl.*) (2003) 209.
- [49] D. B. Cline *et al.* (ZEPLIN-4 Collaboration), *Nucl. Phys.* **124** (*Proc. Suppl.*) (2003) 229.
- [50] Y. Suzuki *et al.* (Xenon Collaboration), [hep-ph/0008296](#).
- [51] See talk by C. Rubbia at 6th UCLA Symposium on *Sources and Detection of Dark Matter and Dark Energy in the Universe*, Marina del Ray, CA, February (2004).

- [52] D. Dicus, S. Nandi and X. Tata, *Phys. Lett.* **B 129** (1983) 451; A. Chamseddine, P. Nath and R. Arnowitt, *Phys. Lett.* **B 129** (1983) 445; H. Baer and X. Tata, *Phys. Lett.* **B 155** (1985) 278; H. Baer, K. Hagiwara and X. Tata, *Phys. Rev. Lett.* **57** (1986) 294 and *Phys. Rev.* **D 35** (1987) 1598; R. Arnowitt and P. Nath, *Mod. Phys. Lett.* **A 2** (1987) 331; R. Barbieri, F. Caravaglios, M. Frigeni and M. Mangano, *Nucl. Phys.* **B 367** (1991) 28; H. Baer and X. Tata, *Phys. Rev.* **D 47** (1993) 2739; J. Lopez, D. Nanopoulos, X. Wang and A. Zichichi, *Phys. Rev.* **D 48** (1993) 2062 and *Phys. Rev.* **D 52** (1995) 142; H. Baer, C. Kao and X. Tata, *Phys. Rev.* **D 48** (1993) 5175; S. Mrenna, G. Kane, G. Kribs and J. Wells, *Phys. Rev.* **D 53** (1996) 1168; H. Baer, C. H. Chen, F. Paige and X. Tata, *Phys. Rev.* **D 54** (1996) 5866.
- [53] V. Barger and C. Kao, *Phys. Rev.* **D 60** (1999) 115015; K. Matchev and D. Pierce, *Phys. Lett.* **B 467** (1999) 225; H. Baer, M. Drees, F. Paige, P. Quintana and X. Tata, *Phys. Rev.* **D 61** (2000) 095007; for a review, see S. Abel *et al.* (SUGRA Working Group Collaboration), hep-ph/0003154
- [54] H. Baer, T. Krupovnickas and X. Tata, *J. High Energy Phys.* **0307** (2003) 020.
- [55] H. Baer, J. Ellis, G. Gelmini, D. V. Nanopoulos and X. Tata, *Phys. Lett.* **B 161** (1985) 175; G. Gamberini, *Z. Physik* **C 30** (1986) 605; H. Baer, V. Barger, D. Karatas and X. Tata, *Phys. Rev.* **D 36** (1987) 96; H. Baer, X. Tata and J. Woodside, *Phys. Rev.* **D 45** (1992) 142.
- [56] H. Baer, C. Balazs, A. Belyaev, T. Krupovnickas and X. Tata, *J. High Energy Phys.* **0306** (2003) 054. For earlier work, see H. Baer, C. H. Chen, F. Paige and X. Tata, *Phys. Rev.* **D 52** (1995) 2746 and *Phys. Rev.* **D 53** (1996) 6241; H. Baer, C. H. Chen, M. Drees, F. Paige and X. Tata, *Phys. Rev.* **D 59** (1999) 055014; S. Abdullin and F. Charles, *Nucl. Phys.* **B 547** (1999) 60; S. Abdullin *et al.* (CMS Collaboration), hep-ph/9806366; B. Allanach, J. Hetherington, A. Parker and B. Webber, *J. High Energy Phys.* **08** (2000) 017.
- [57] H. Baer, R. Munroe and X. Tata, *Phys. Rev.* **D 54** (1996) 6735.
- [58] H. Baer, A. Belyaev, T. Krupovnickas and X. Tata, *J. High Energy Phys.* **0402** (2004) 007 and hep-ph/0405058.
- [59] J. Navarro, C. S. Frenk and S. D. M. White, *Astrophys. J.* **462** (1996) 563.
- [60] B. Moore, F. Governato, T. Quinn, J. Stadel and G. Lake, *Astrophys. J.* **499** (1998) L5.
- [61] A. V. Kravtsov, A. Klypin, J. Bullock and J. Primack, astro-ph/9708176.
- [62] S. Profumo and P. Ullio, *JCAP***0311** (2003) 006.
- [63] See H. Baer and M. Brhlik, Ref. [9].
- [64] H. Baer, C. H. Chen, M. Drees, F. Paige and X. Tata, *Phys. Rev. Lett.* **79** (1997) 986.
- [65] See H. Baer, C. Balazs, A. Belyaev and J. O’Farrill, Ref. [16]
- [66] J. Edsjö, M. Schelke and P. Ullio, astro-ph/0405414.

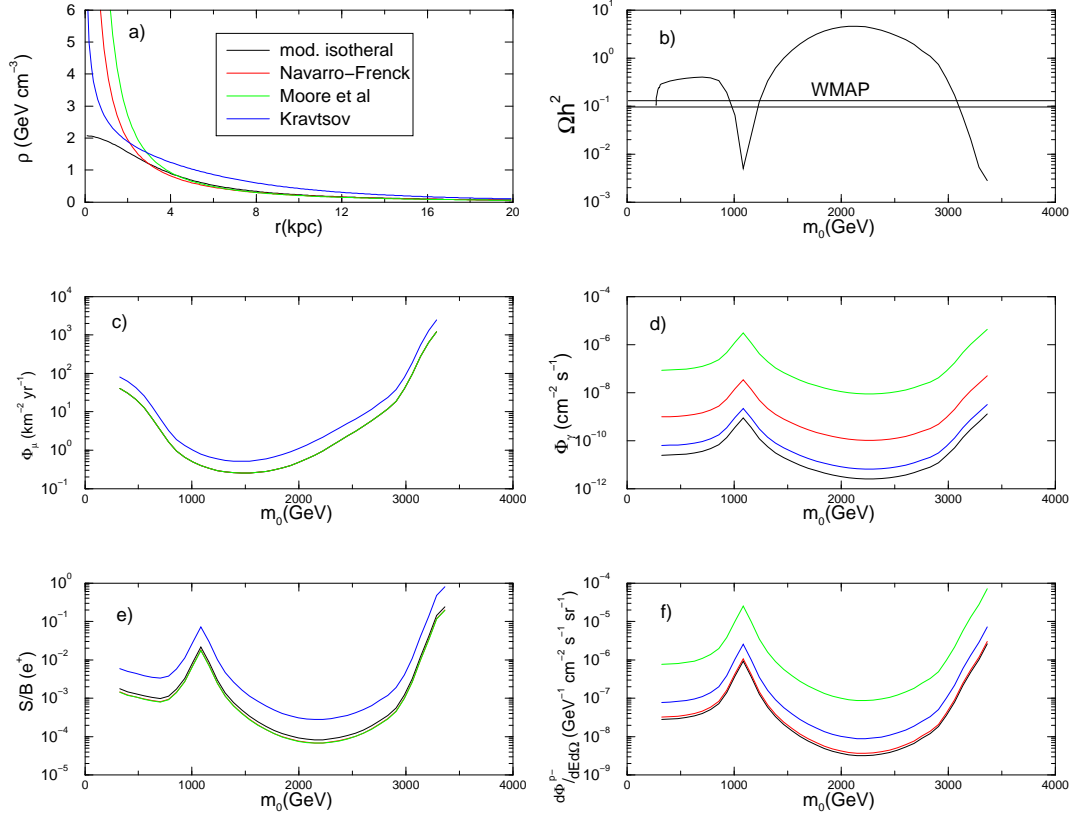


Figure 1: In frame *a*), we show various halo model density profiles versus galactic radial distance r (kpc), while in frame *b*), we show the neutralino relic density, along with the WMAP bound (horizontal line). Frame *c*) shows the flux of muons from the sun. In frames *d*), *e*), and *f*) we show rates for detection of γ s, e^+s and $\bar{p}s$ from neutralino annihilations in the galactic core and halo, for different halo model choices. Frames *b*)–*f*) are plotted versus m_0 for $m_{1/2} = 550$ GeV, $A_0 = 0$, $\tan\beta = 50$ and $\mu < 0$.

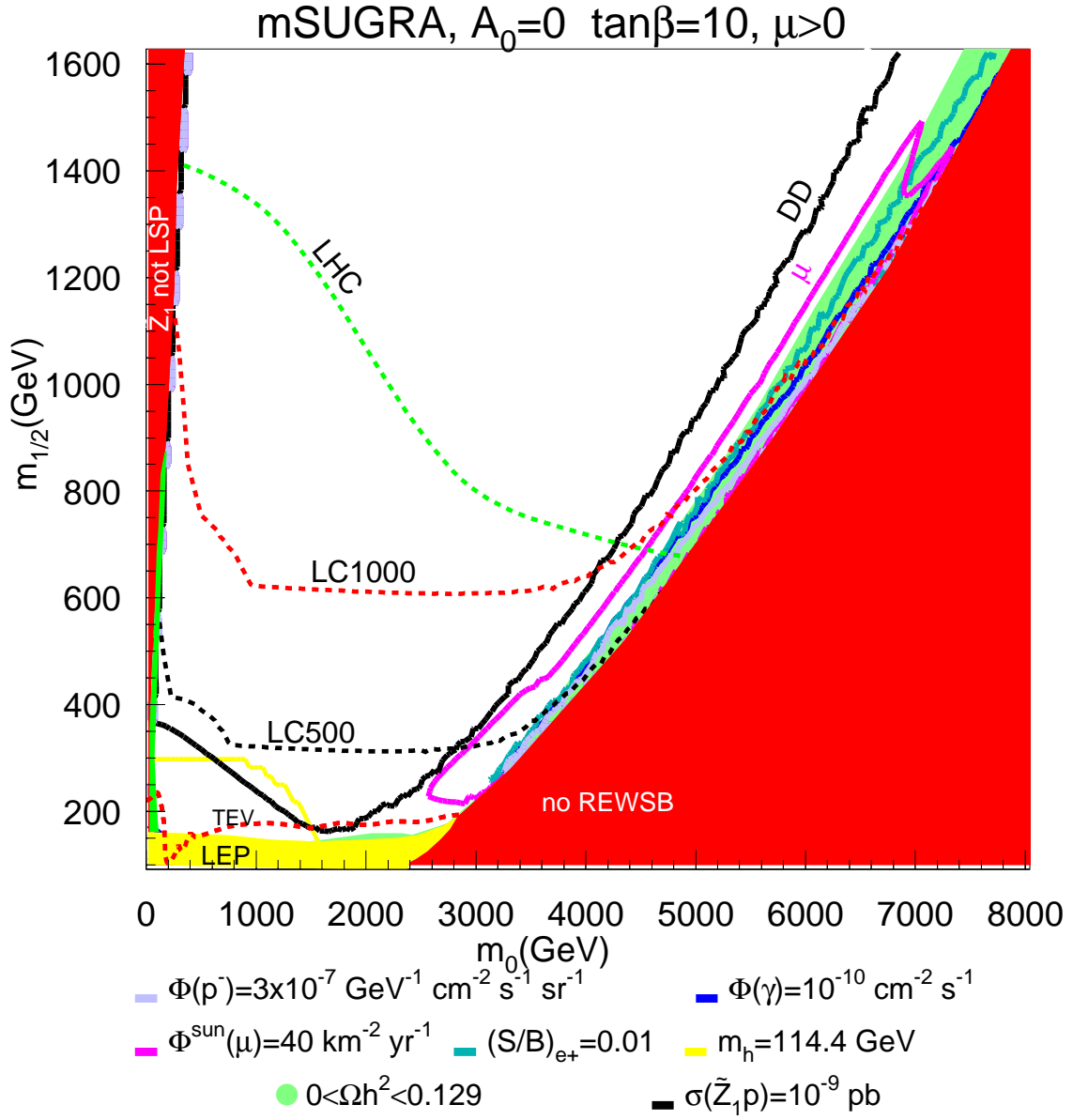


Figure 2: A plot of the reach of direct, indirect and collider searches for neutralino dark matter in the m_0 vs. $m_{1/2}$ plane, for $A_0 = 0$, $\tan\beta = 10$ and $\mu > 0$.

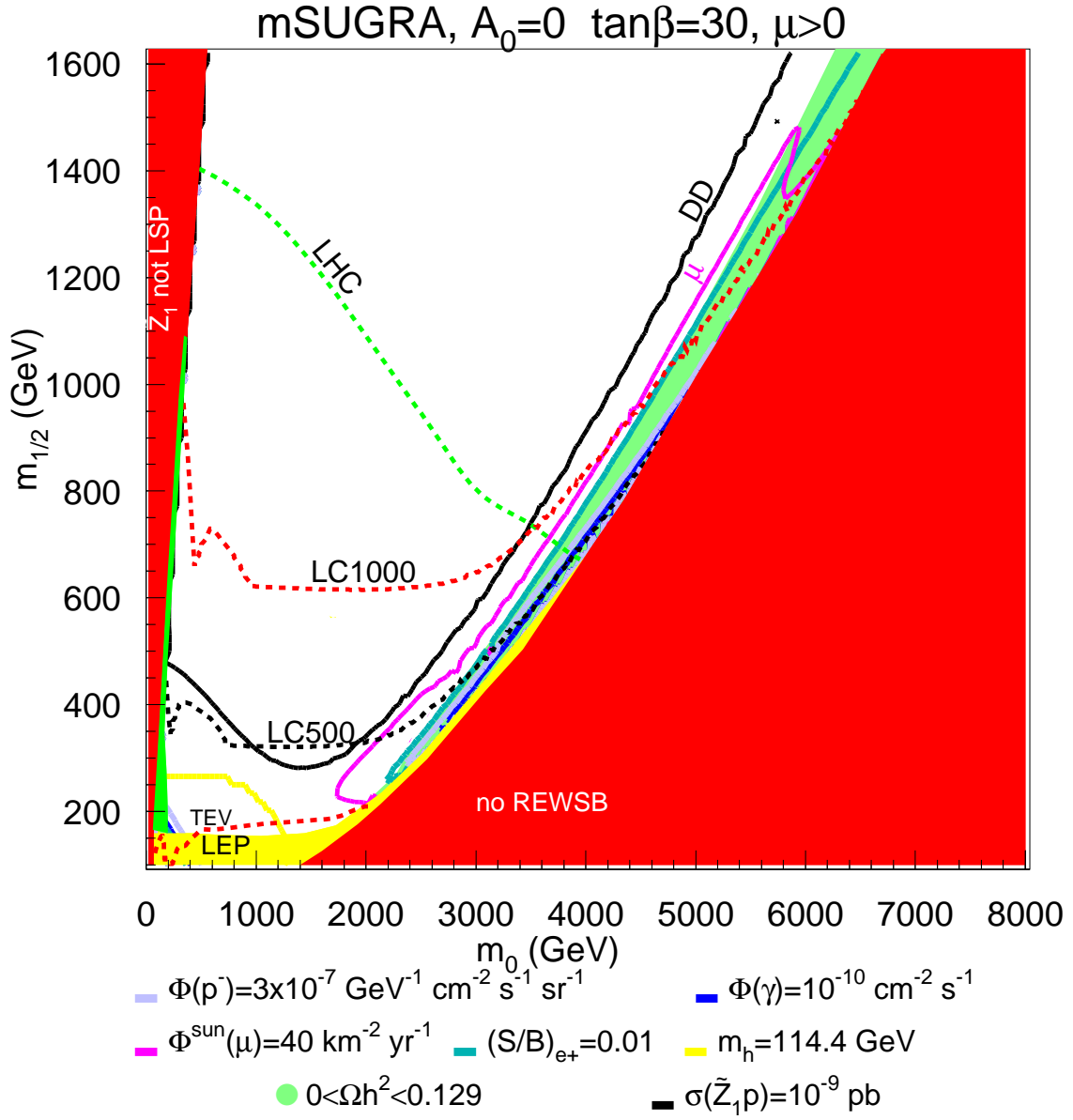


Figure 3: A plot of the reach of direct, indirect and collider searches for neutralino dark matter in the m_0 vs. $m_{1/2}$ plane, for $A_0 = 0$, $\tan\beta = 30$ and $\mu > 0$.

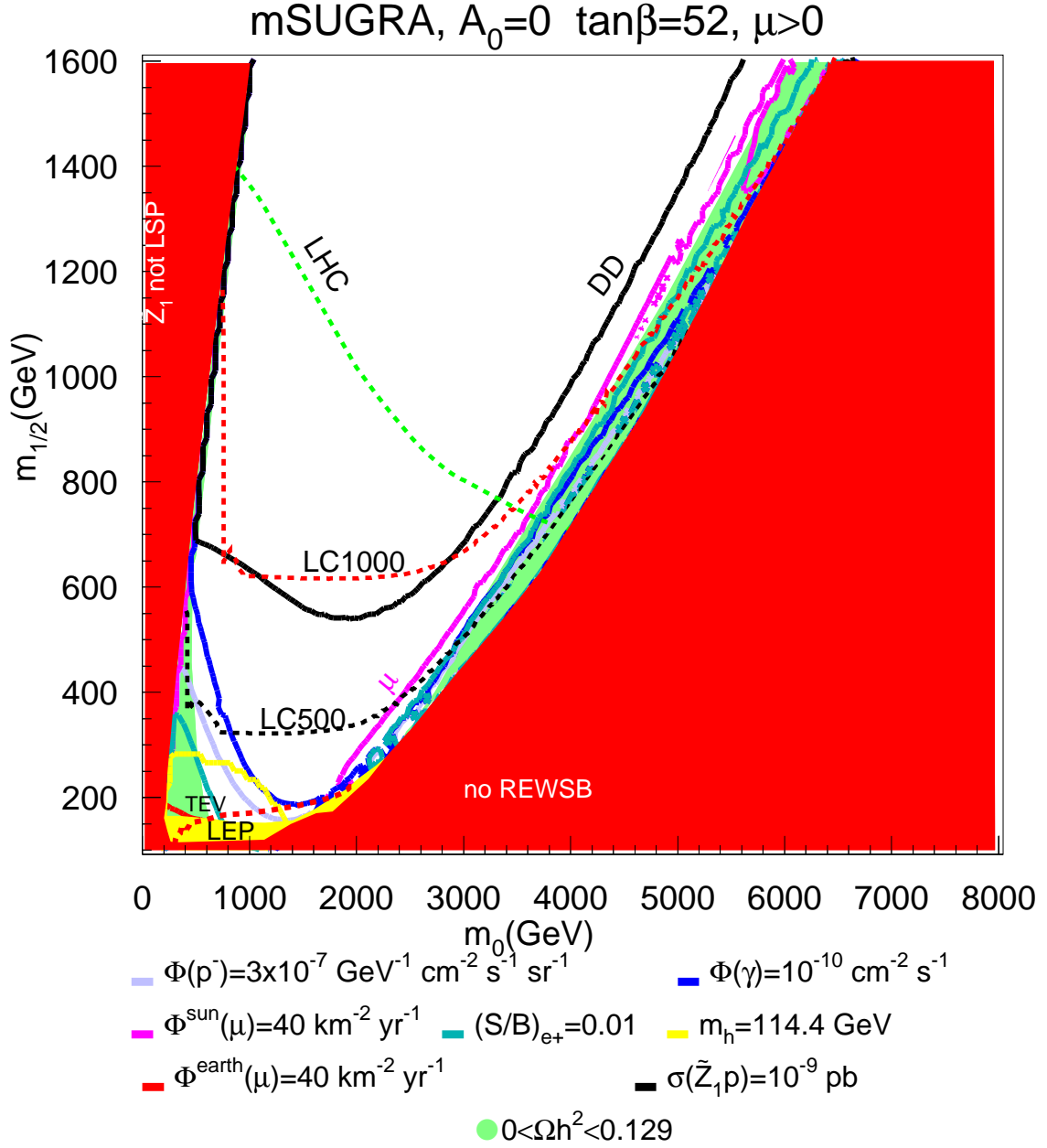


Figure 4: A plot of the reach of direct, indirect and collider searches for neutralino dark matter in the m_0 vs. $m_{1/2}$ plane, for $A_0 = 0$, $\tan\beta = 52$ and $\mu > 0$.

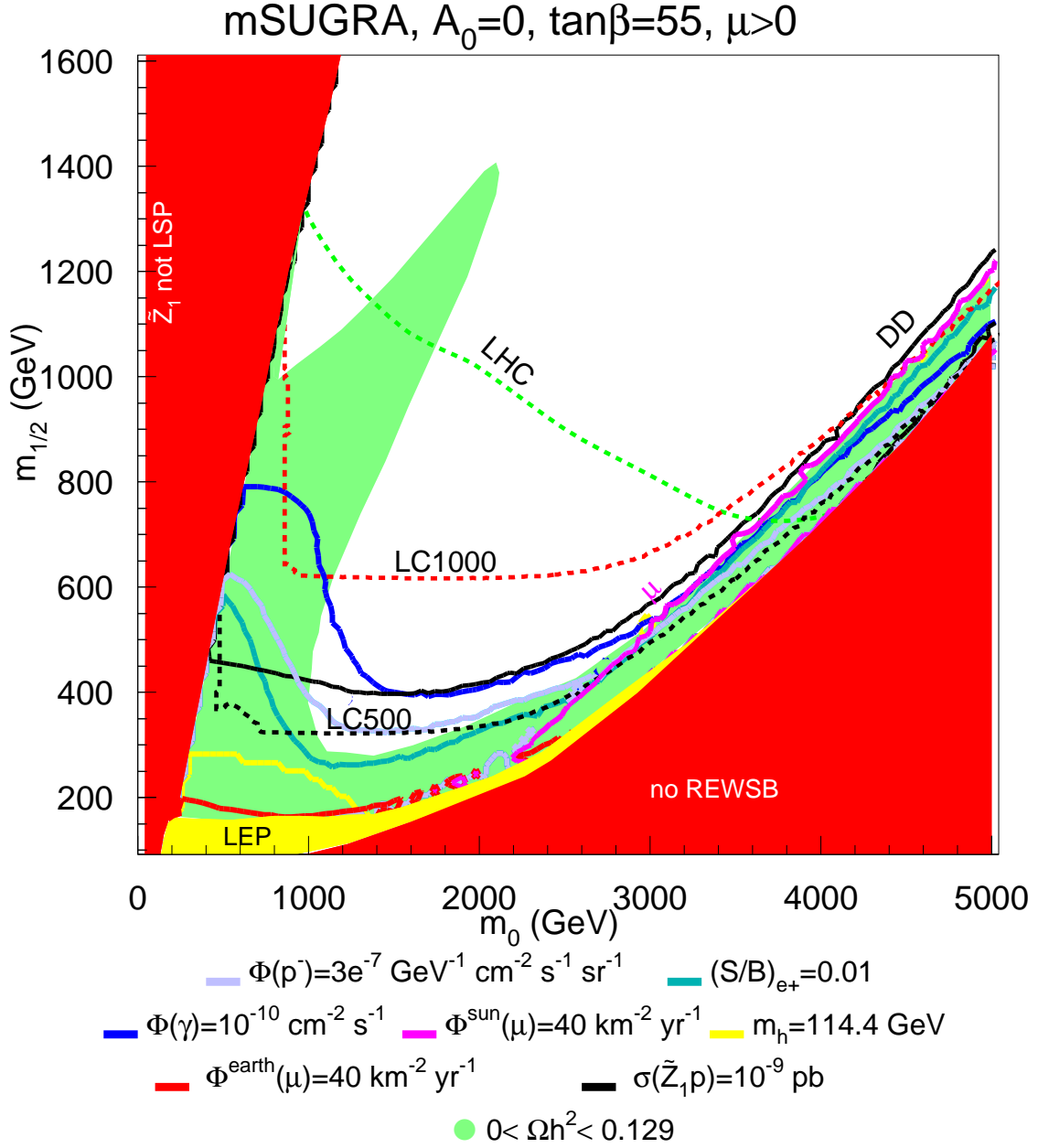


Figure 5: A plot of the reach of direct, indirect and collider searches for neutralino dark matter in the m_0 vs. $m_{1/2}$ plane, for $A_0 = 0$, $\tan\beta = 55$ and $\mu > 0$.

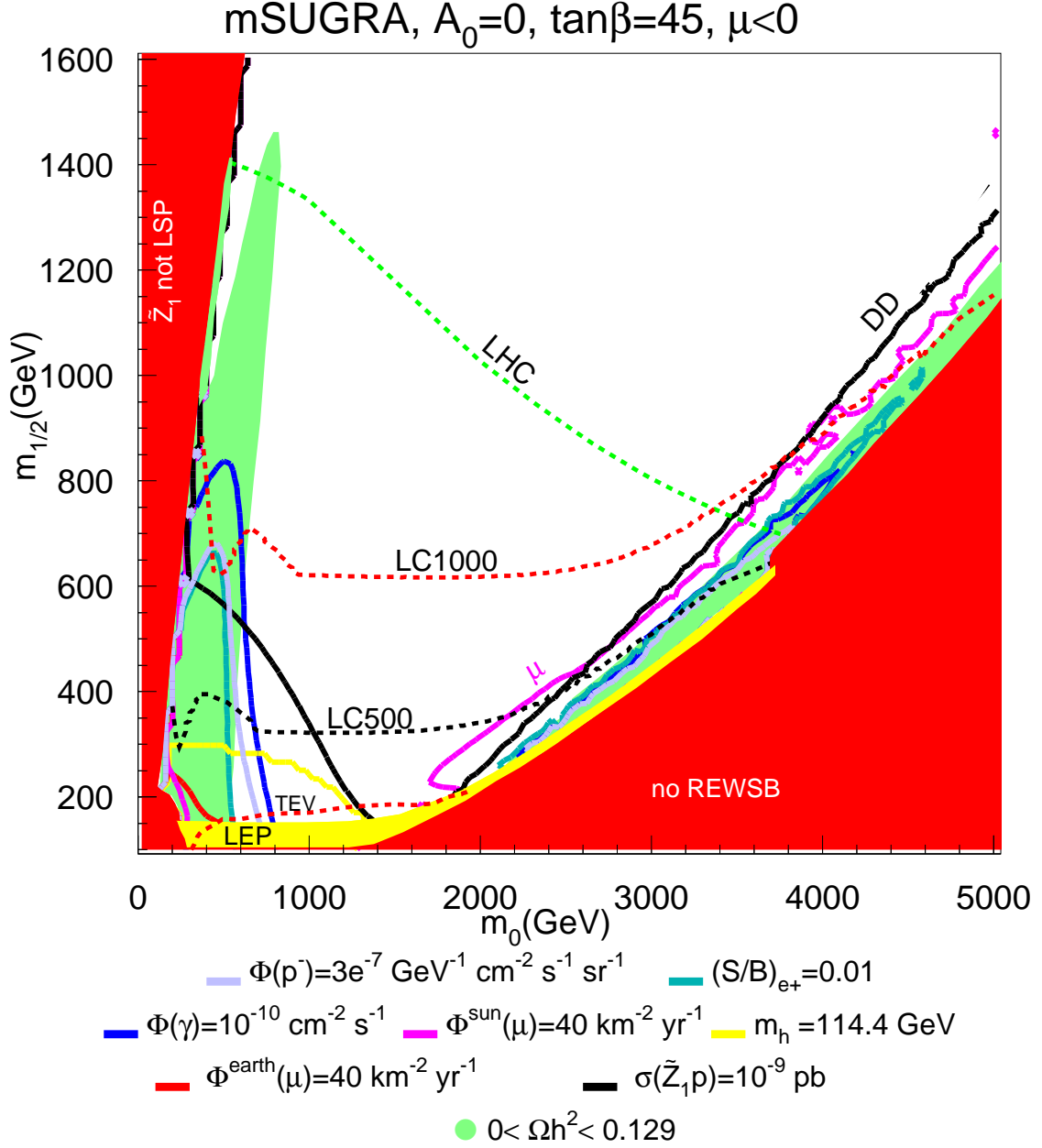


Figure 6: A plot of the reach of direct, indirect and collider searches for neutralino dark matter in the m_0 vs. $m_{1/2}$ plane, for $A_0 = 0$, $\tan\beta = 45$ and $\mu < 0$.

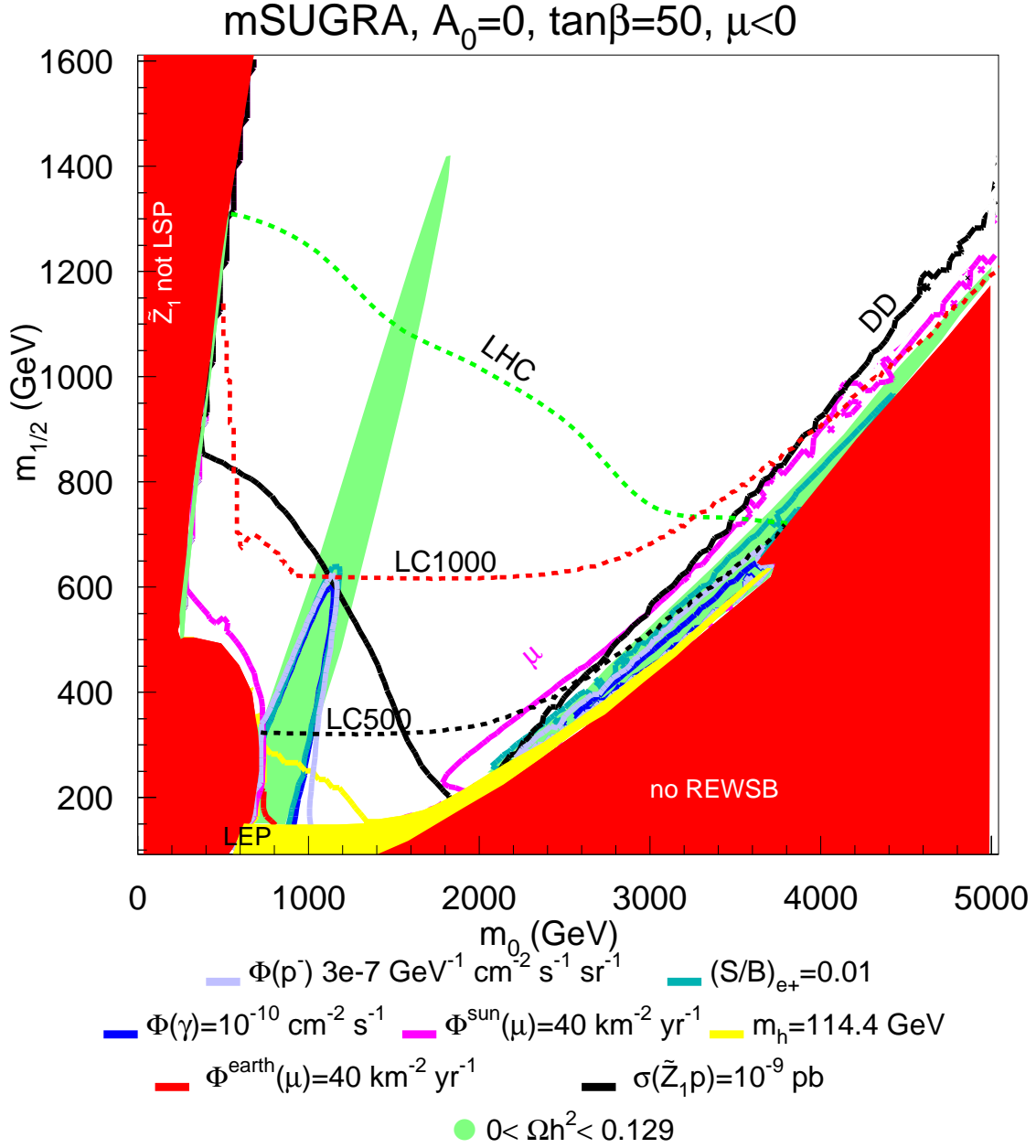


Figure 7: A plot of the reach of direct, indirect and collider searches for neutralino dark matter in the m_0 vs. $m_{1/2}$ plane, for $A_0 = 0$, $\tan\beta = 50$ and $\mu < 0$.